

1  
2 *Elementa: Science of the Anthropocene*

3 Supplemental Material for

4 **Insights on Sources and Formation Mechanisms of Liquid-Bearing Clouds over**  
5 **MOSAiC Examined from a Lagrangian Framework**

6 **Israel Silber<sup>1</sup> and Matthew D. Shupe<sup>2,3</sup>**

7  
8  
9  
10 [1] Department of Meteorology and Atmospheric Science, Pennsylvania State University, University  
11 Park, Pennsylvania, USA

12 [2] Cooperative Institute for Research in Environmental Science, Boulder, Colorado, USA

13 [3] NOAA/Physical Sciences Laboratory, Boulder, Colorado, USA

14  
15 Correspondence to: Israel Silber (ixs34@psu.edu)

16  
17  
18  
19  
20 **January 2022**

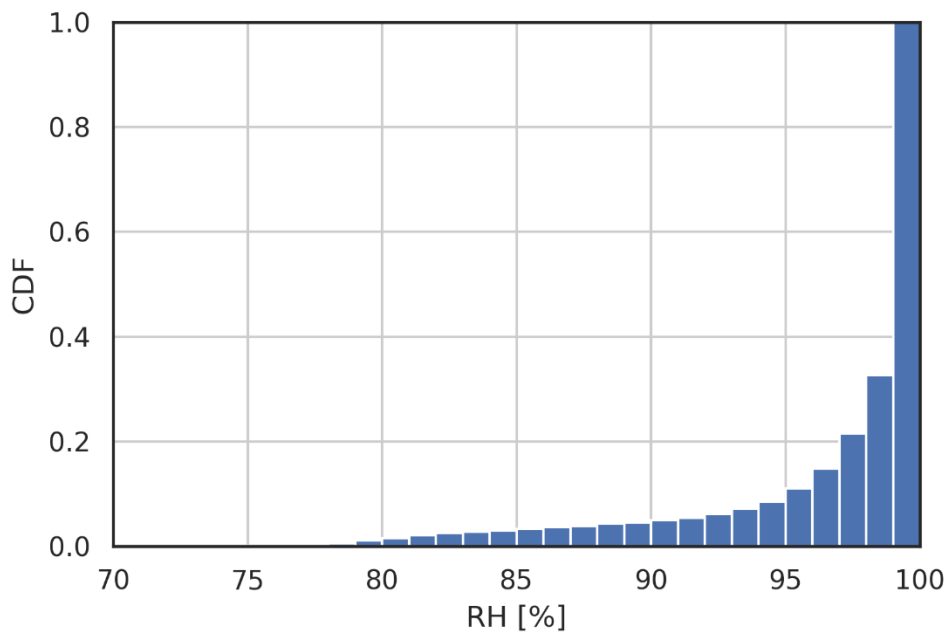
1 **Contents of this file**

2 Figures S1 and S2

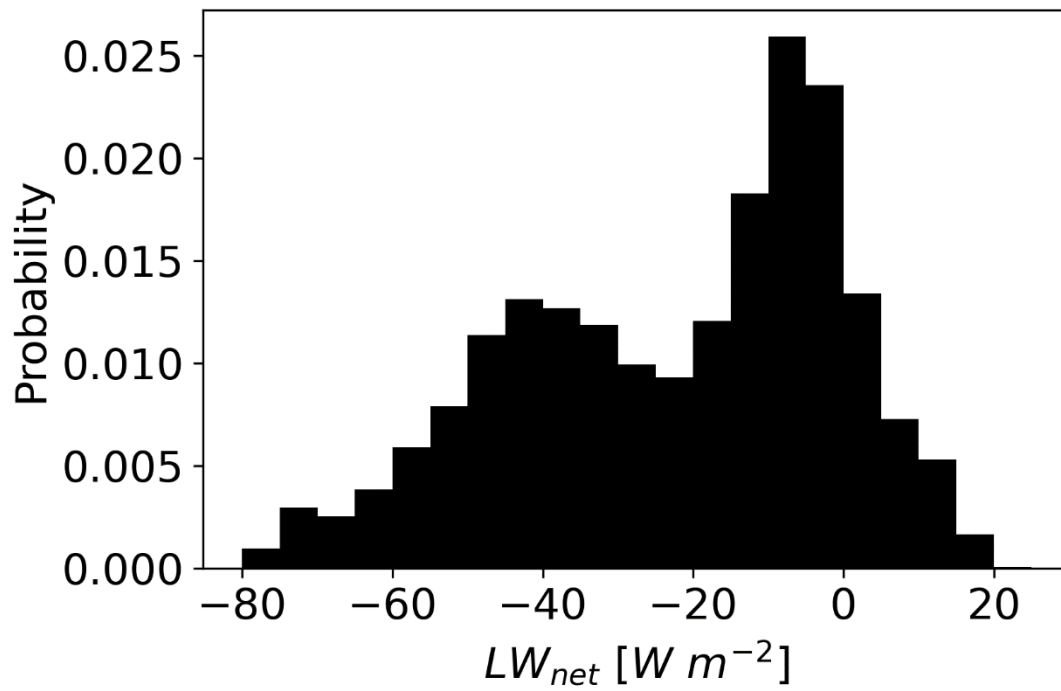
3 **Introduction**

4 The supplemental material includes 2 figures:

- 5 • **Figure S1** depicts the cumulative distribution function of relative humidity (RH) from  
6 sounding measurements at high spectral resolution lidar (HSRL) liquid cloud base heights.
- 7 • **Figure S2** shows the net surface longwave radiation ( $LW_{\text{net}}$ ) histogram for the full MOSAiC  
8 deployment.



2 **Figure S1: Cumulative distribution function of relative humidity (RH) from sounding**  
3 **measurements at high spectral resolution lidar (HSRL) liquid cloud base heights (LCBHs; [Silber](#)**  
4 **[et al., 2021](#)) (N = 29,375). For this comparison, all LCBH detections up to 15 min following**  
5 **radiosonde release times are used, while excluding LCBHs at temperatures between -20 and -8**  
6 **°C, thereby mitigating the potential influence of specular reflection artifacts in the HSRL data**  
7 **(see [Silber et al., 2018](#), Appendix A). The 15 min window covers the radiosonde ascent up to ~4.3**  
8 **km, and hence, generally represents the vast majority of liquid-bearing clouds detected over**  
9 **MOSAiC (see Figure 3c in the text). More than 85% of all HSRL LCBH detections correspond**  
10 **with RH values greater than 96% (liquid-bearing cloud detection threshold used in the text).**  
11 **[Silber et al., \(2018\)](#) have demonstrated that the HSRL LCBH algorithm typically determines the**  
12 **LCBH just above the level of aerosol deliquescence. This algorithm property combined with the**  
13 **RS-41 radiosonde RH measurement response time of a few to several seconds at sub-freezing**  
14 **temperatures (see [Holdridge, 2020](#)) could explain, in addition to the influence of different probed**  
15 **HSRL and sounding regions, the remaining 15% of samples in which RH is high but smaller**  
16 **than 96%.**



2 **Figure S2: Net surface longwave radiation ( $LW_{net}$ ) histogram for the full MOSAiC deployment**  
3 **based on measurements from the central observatory (see text; bin width of  $5 W m^{-2}$ ). The**  
4 **“radiatively cloudy” state threshold discussed in the text is determined based on the histogram’s**  
5 **local minimum at  $-25 W m^{-2}$ .**